Test and Evaluation Report

Testing and Evaluation of the Iowa DOT FRP Temporary Bypass Bridge

November 22, 2005

Prepared For

Iowa Department of Transportation

Iowa Department of Transportation
Office of Bridges and Structures
800 Lincoln Way
Ames, IA 50010

Prepared By

BRIDGE ENGINEERING CENTER

Bridge Engineering Center
2901 South Loop Dr.
Suite 3100
Ames, IA 50010
(515) 294-8103

Introduction

On November 7 and 14, 2005 the FRP temporary bypass bridge owned by the Iowa Department of Transportation was tested (Test 1 and Test 2, respectively) using a fully loaded Iowa Department of Transportation tandem axle dump truck which was statically placed on the structure in the three load positions listed below (in all cases the load truck was positioned longitudinally for maximum moment, facing north):

- Load Case 1 – passenger side wheel 2' from face of east guardrail
- Load Case 2 – truck transversely centered on bridge
- Load Case 3 – driver side wheel 2' from face of west guardrail

Note: The guardrail was not yet placed at the time of testing.

Test 2 was conducted after evaluating the Test 1 data to clarify some observations and included fewer (and, in some cases different) instrumentation locations than used in Test 1 see; Fig. 1 and 2 for instrumentation layouts. Strain data were collected on the top and bottom of the deck panels near mid-span of the 39' 10" long panels (Test 1 and 2), and on the bottom only at the quarter-span of the panels on the south half (Test 1 only). In addition, deflection data were collected at the mid-span of the panels (Test 1 only). The collected strain and deflection data are the basis of the results and conclusions made herein. For reference, the gages are numbered from east to west (i.e. looking south). Top and bottom gages are specified in the text below with a (T) and (B), respectively.

Test Results

Table 1 lists the Test 1 mid-span deflections for the three load positions. The maximum measured deflection for any given load case was 0.34 in., which is less than the deflection limit of L/800 or 0.59 in. The L/800 criteria is based on H-20 loading, which is a 40,000 lb truck; our test trucks were 44,350 lb and 44,740 lb (Test 1 and 2, respectively), so the presented data are conservative.

Illustrated in Figure 3 is the strain profile for the top and bottom gages at mid-span for load case 2 (LC2) for Test 1, which is a symmetrical transverse truck position, and is generally representative of all three load cases for Test 1. The overall response is symmetric except at SG6 (T), near the west edge of the bridge. The generally symmetric behavior suggests a neutral axis near mid-depth of the panel (as would be expected) across the width of the bridge. Figure 4 compares top (T) panel strains at gages SG1, SG3, SG4 and SG6 for Test 1 with corresponding strains from gages SG2, SG3, SG4 and SG5 for Test 2 across the transverse mid-span for LC3. From Fig. 4, it would appear that the strain measured at SG6 (T) for the Test 1 is suspect. It is unclear whether this is due to localized effects from the close proximity of the rear axles, gage bonding issues, or other effects.

For Test 2, an additional gage was installed on the top of the panel approximately 1ft south of gages SG1 and SG6, to validate the measured strains from Test 1. Illustrated in Fig. 5 are the top strains measured at gages SG6 for Test 1, and SG5 and SG6 for Test 2

for all three load cases. Combined, the data further suggest that the data obtained from gage SG6 (T) during Test 1 may be incorrect as noted above. Replacing the measured strain at SG6 for Test 1 with the measured strain at SG5 for Test 2, a more symmetric top and bottom strain profile is obtained, as shown in Fig. 6.

Figures 7 and 8 illustrate the transverse distribution of strain at mid-span for a single lane loaded and two lanes loaded, respectively (similar transverse distribution was calculated at quarter-span but is not shown here). The two lanes loaded case was approximated by superposition of LC 1 and 3. As shown, it is evident that the distribution of strain is relatively symmetric about the longitudinal centerline of the bridge, which suggests adequate load transfer from panel to panel by the steel connection plates. Note that SG7 strain data are not shown in Fig. 7 or 8. These data represent the strain on the steel connection plates. Generally, the flexural strain measured in the steel connection plates were smaller in magnitude than those in the FRP, possibly the result of slip occurring between the connection plate and the panels as well as other factors.

Presented in Table 2 are mid-span strain values for LC 1 – 3 for Test 1. Maximum tensile strains (microstrain) recorded in the FRP for each load case were: LC1 1 – 171, LC2 – 130, and LC3 – 179. Assuming a modulus of elasticity of 4,000 ksi, these maximum recorded strains are equivalent to a stress of approximately 0.68 ksi, 0.52 ksi, and 0.72 ksi, respectively. For the two lanes loaded case the maximum strain value (microstrain) is approximately 254, which is equivalent to a stress of 1.01 ksi. Maximum recorded strains (microstrain) in the steel for each load case were: LC2 – 51, LC2 – 8, and LC3 – 27. Assuming a modulus of elasticity of 29,000 ksi, these maximum strains are equivalent to a stress of approximately 1.48 ksi, 0.23 ksi, and 0.78 ksi, respectively.

From Fig. 3 and 6, it is evident that, for the most part, the neutral axis is near mid depth of the panels. A similar approximation of the neutral axis was not as consistent when using strains measured on the side of the panels. Three vertical cross-sections were instrumented on both the East and West side of the bridge (1ft south of centerline, centerline, and 2 ft north of centerline), with four gages vertically symmetrically placed at each cross-section. Figures 9 and 10 illustrate the vertical strain distribution at each location for the East and West sides, respectively for LC2 which is representative of all load cases. The figures suggest that there are differences in the neutral axis location from cross section to cross section, likely a result of the non-homogeneous nature of the materials/bridge.

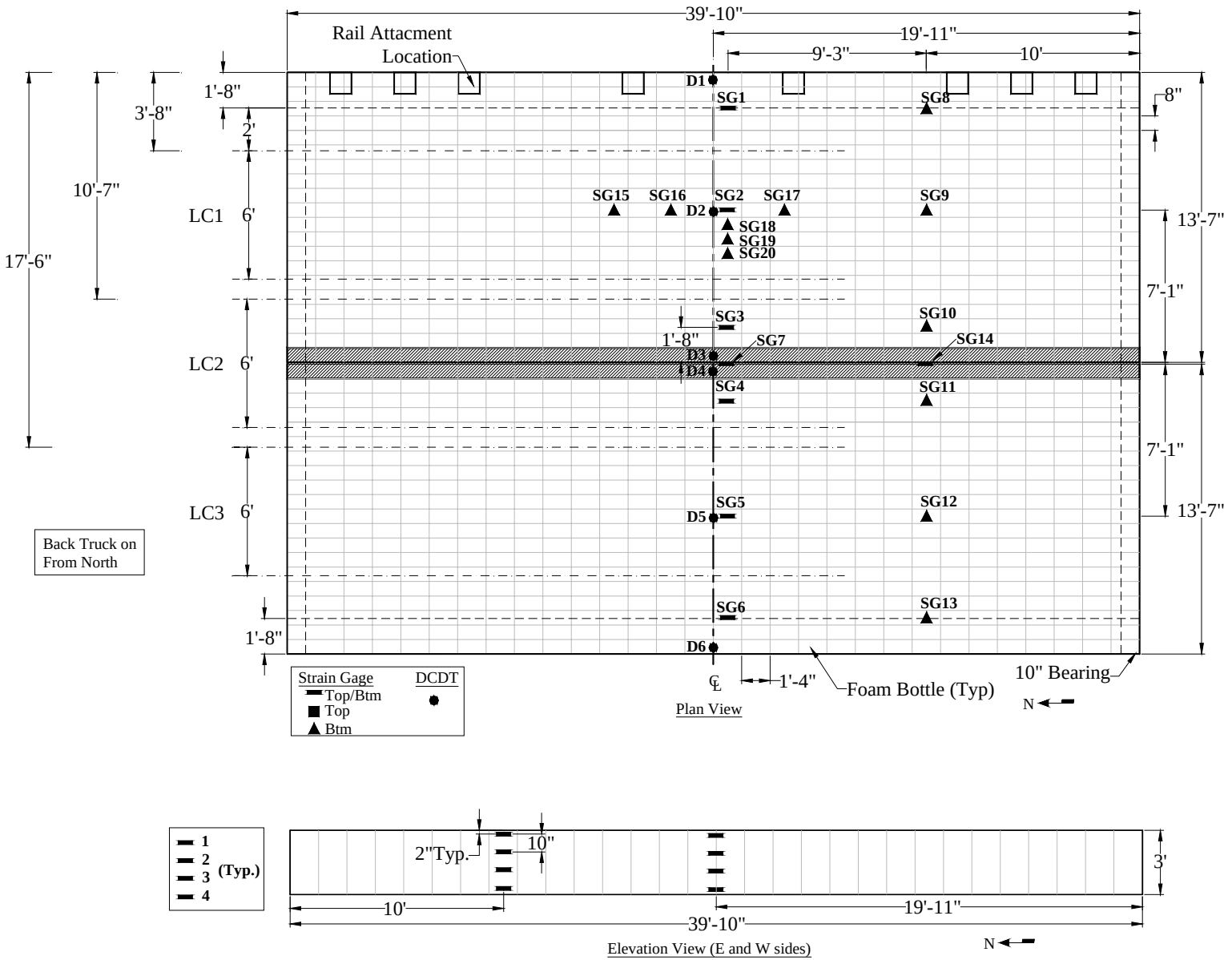

Figure 1. Instrumentation layout, Test 1, FRP Deck Bridge (vehicle facing north).

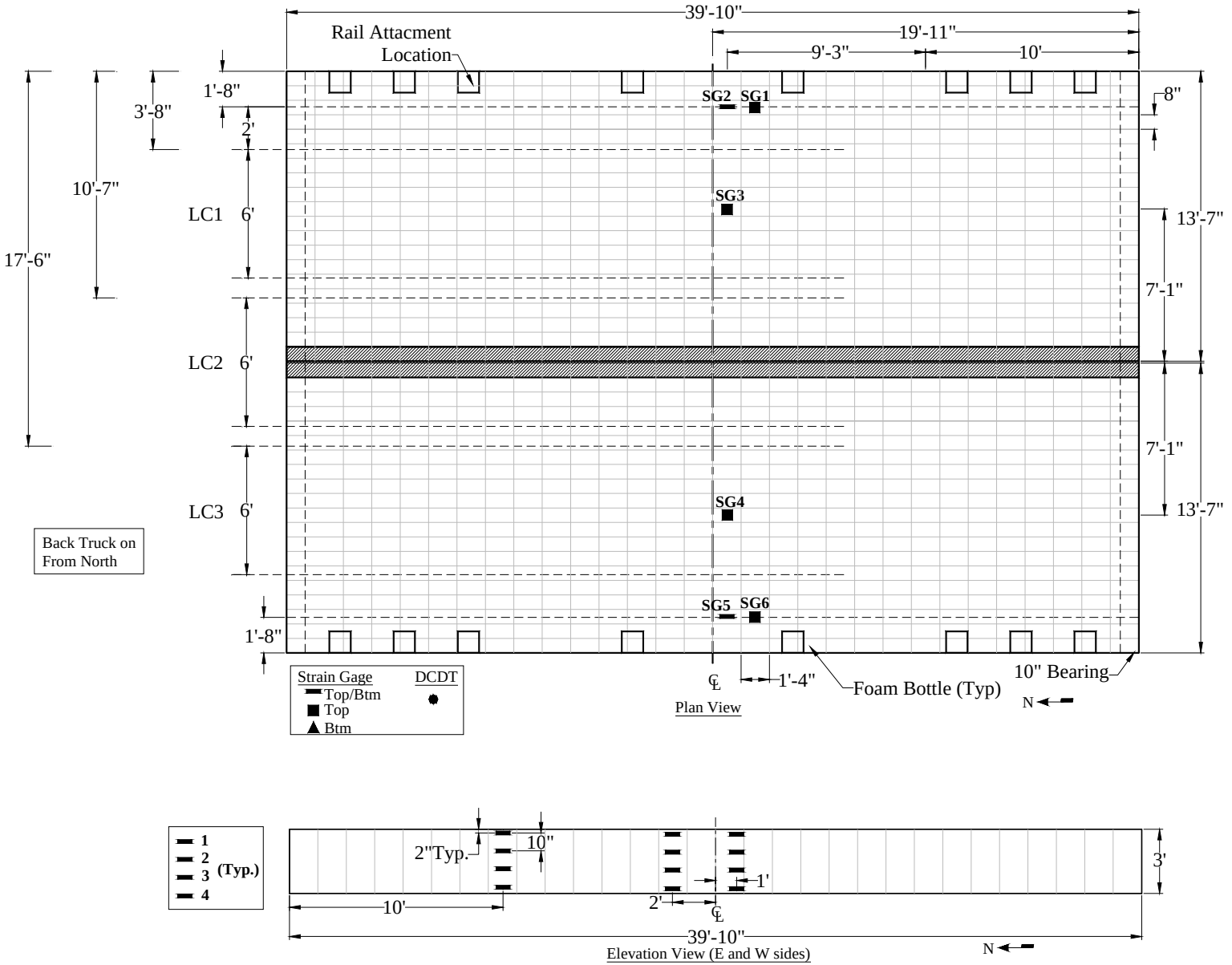

Figure 2. Instrumentation layout, Test 2, FRP Deck Bridge (vehicle facing north).

Table 1. Mid-span Deflections (in.) for Test 1.

	D1	D2	D3	D4	D5	D6
LC1	-0.34	-0.28	-0.23	-0.17	-0.13	-0.07
LC2	-0.17	-0.21	-0.26	-0.25	-0.21	-0.17
LC3	-0.07	-0.13	-0.22	-0.25	-0.30	-0.34

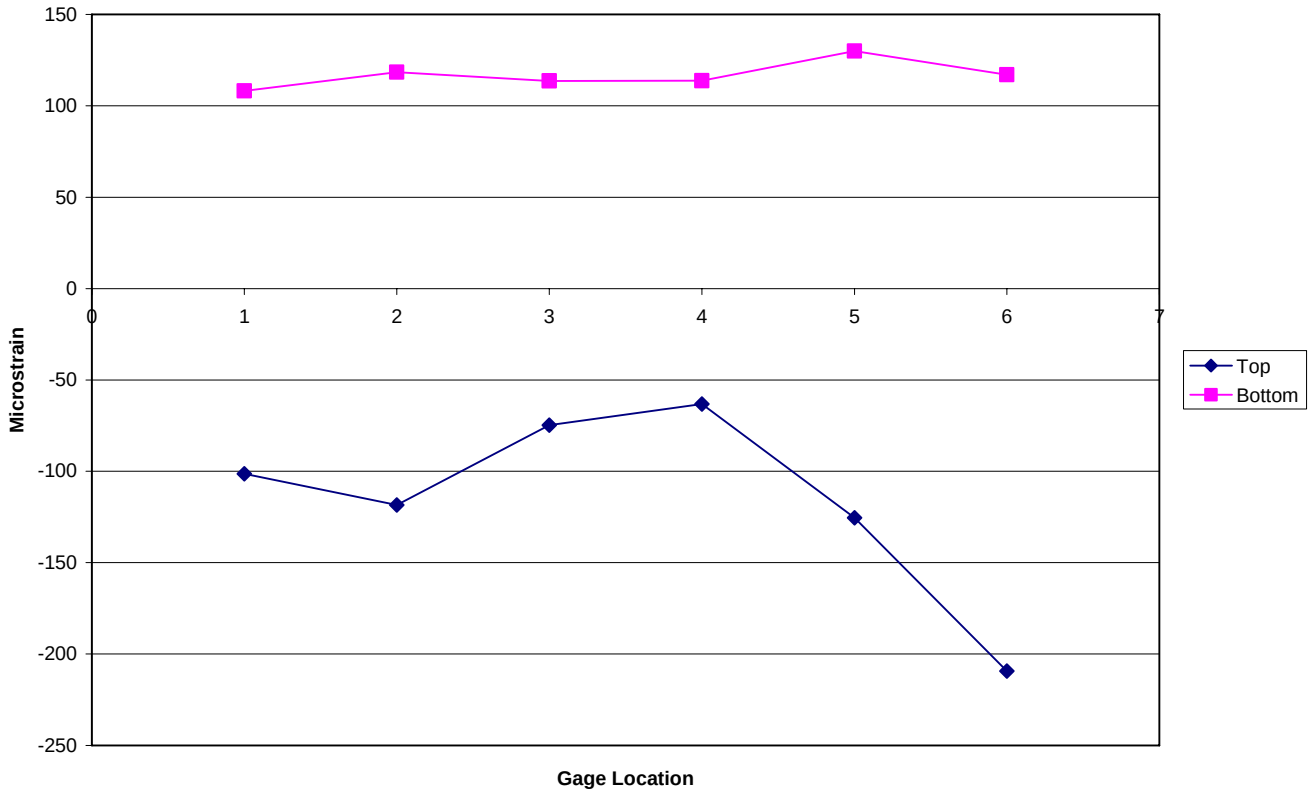

Figure 3. Top and Bottom strain profile at mid-span, LC2.

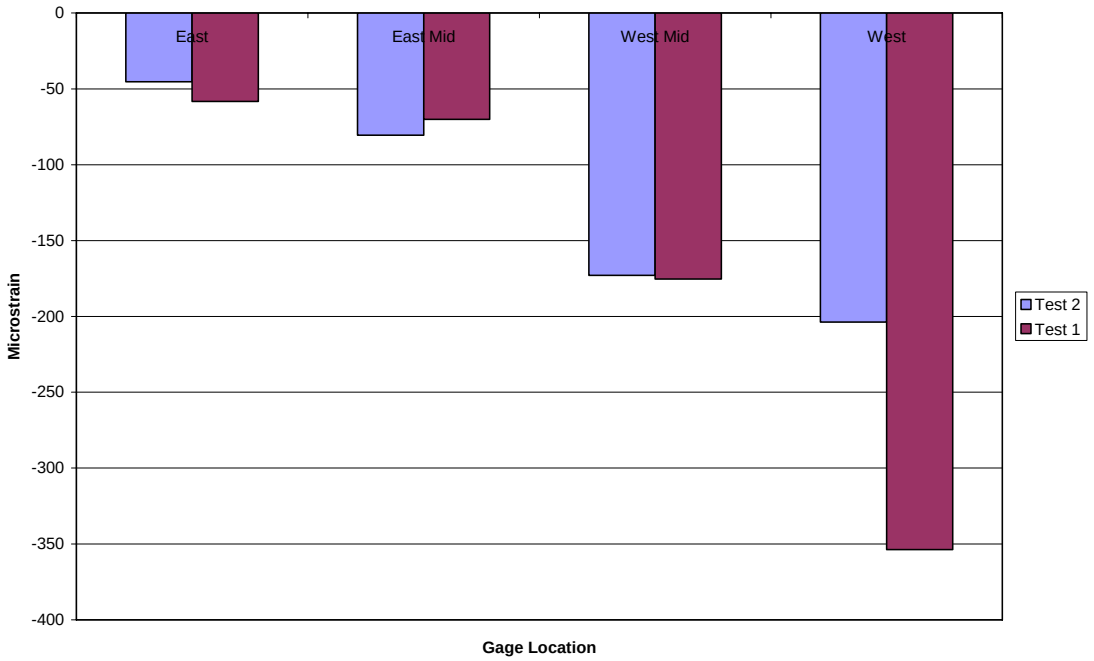

Figure 4. Top panel strain correlation, LC3, Test 1 and 2.

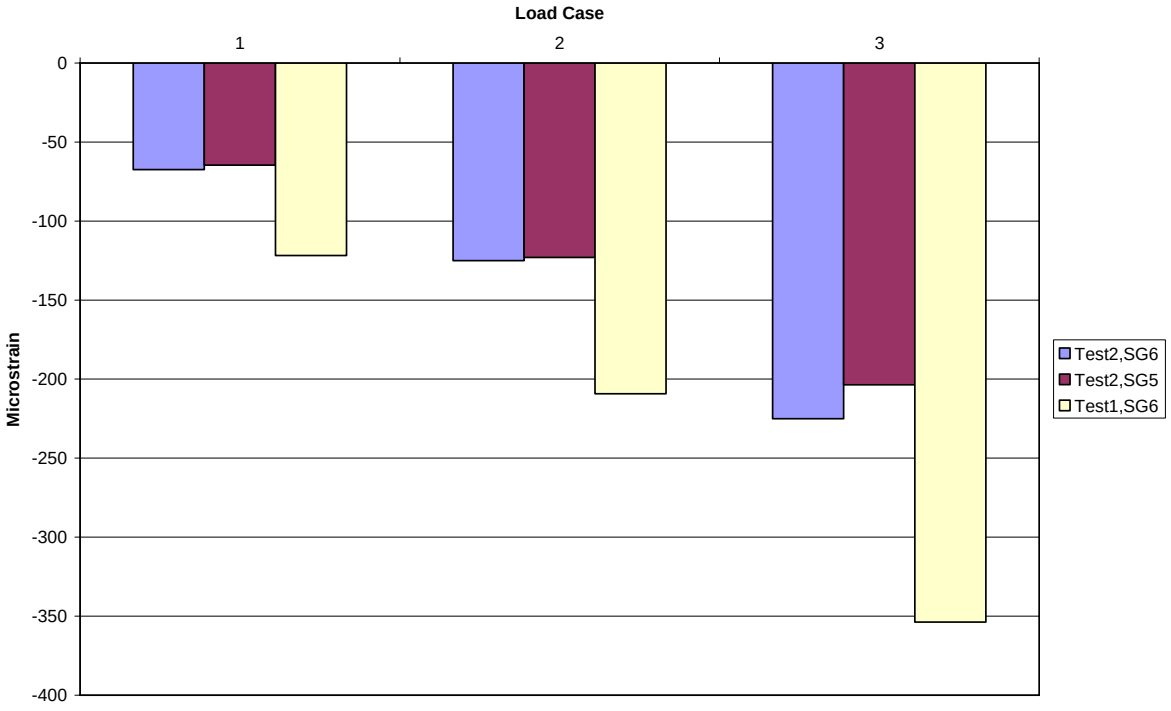

Figure 5. Strain comparison near SG6, Tests 1 and 2.

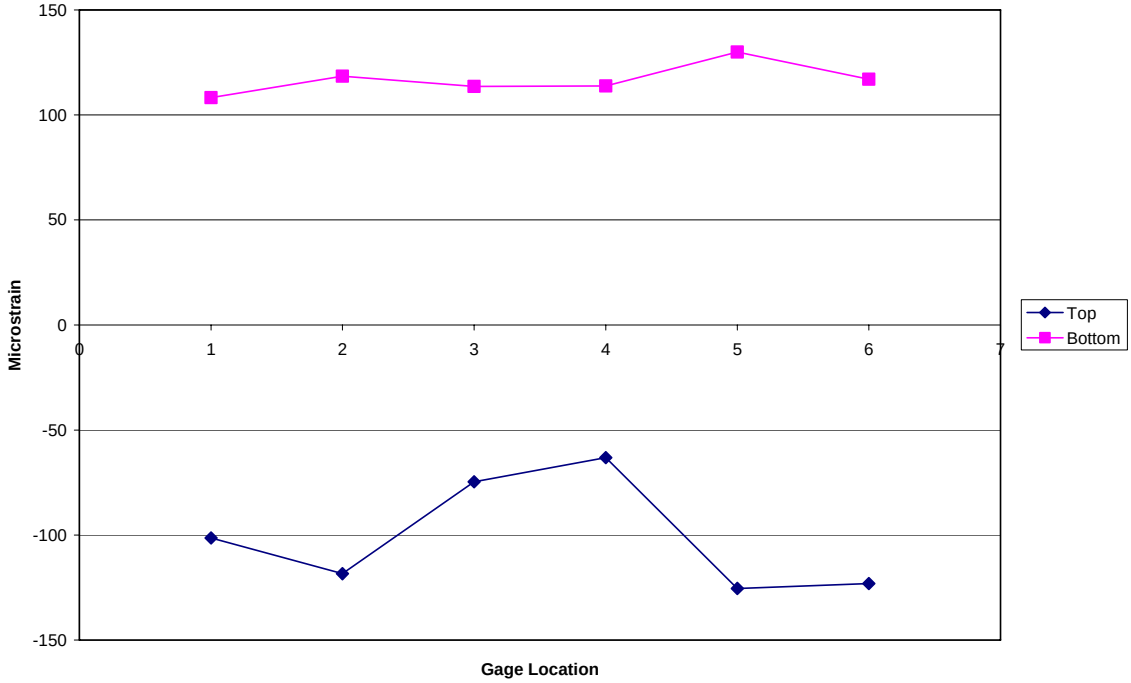

Figure 6. Top and Bottom strain profile at mid-span, LC2; SG6 adjusted with Test 2 data.

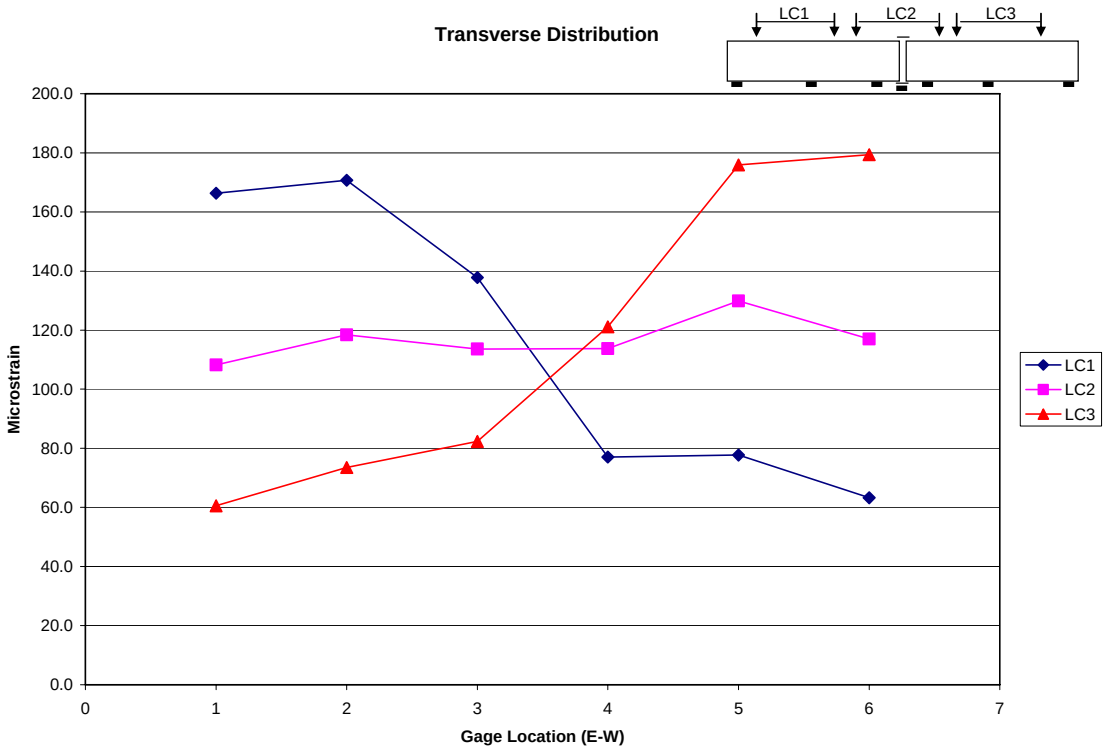

Figure 7. Transverse load distribution at mid-span for all three load cases.

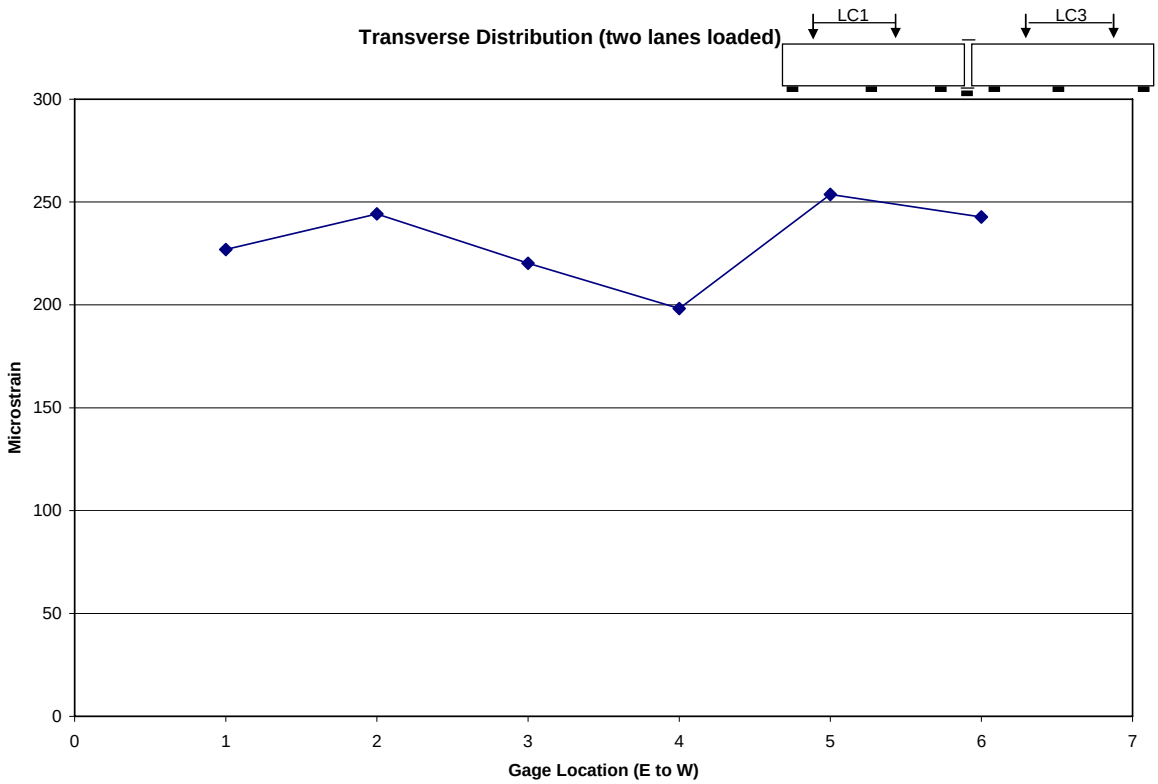

Figure 8. Transverse load distribution at mid-span, two lanes loaded.

Table 2. Top and Bottom Strain Values for LC 1 – 3 at mid-span (microstrain) for Test 1.

LC1	SG1	SG2	SG3	SG7 (steel)	SG4	SG5	SG6
Top	-182	-180	-86	-51	-80	-76	-122
Bottom	166	171	138	24	77	78	63
LC2	SG1	SG2	SG3	SG7 (steel)	SG4	SG5	SG6
Top	-101	-118	-75	-8	-63	-125	-209
Bottom	108	118	114	-7	114	130	117
LC3	SG1	SG2	SG3	SG7 (steel)	SG4	SG5	SG6
Top	-58	-70	-40	27	-92	-175	-354
Bottom	61	74	82	-25	121	176	179

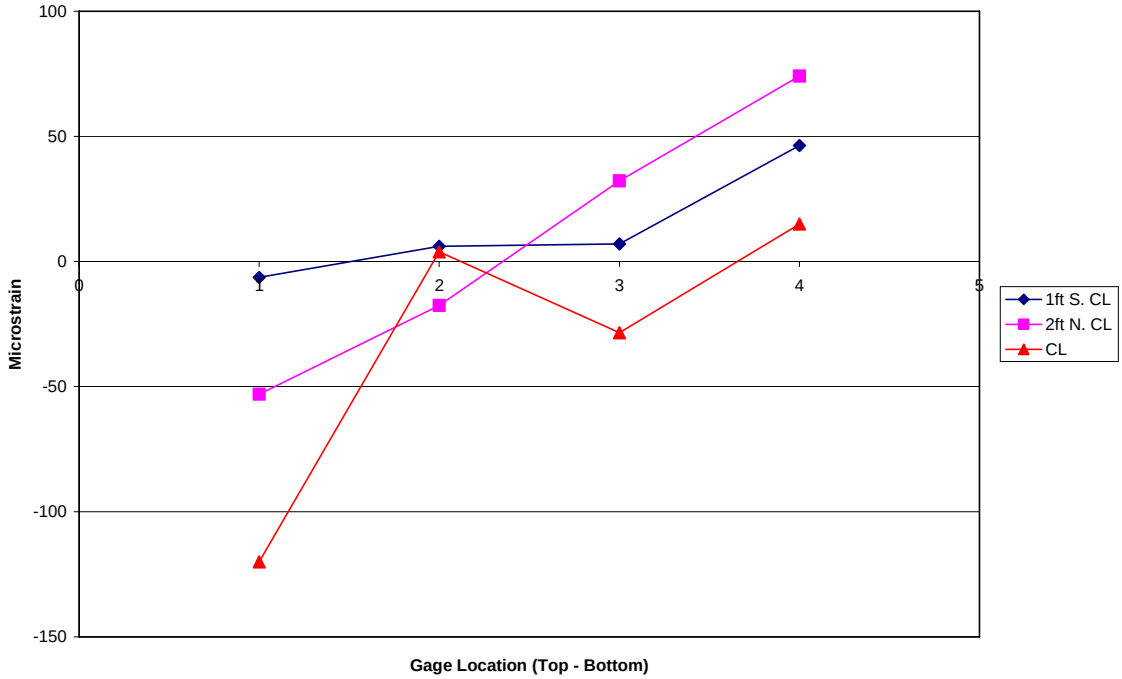

Figure 9. Side panel strain distribution, East side, LC2.

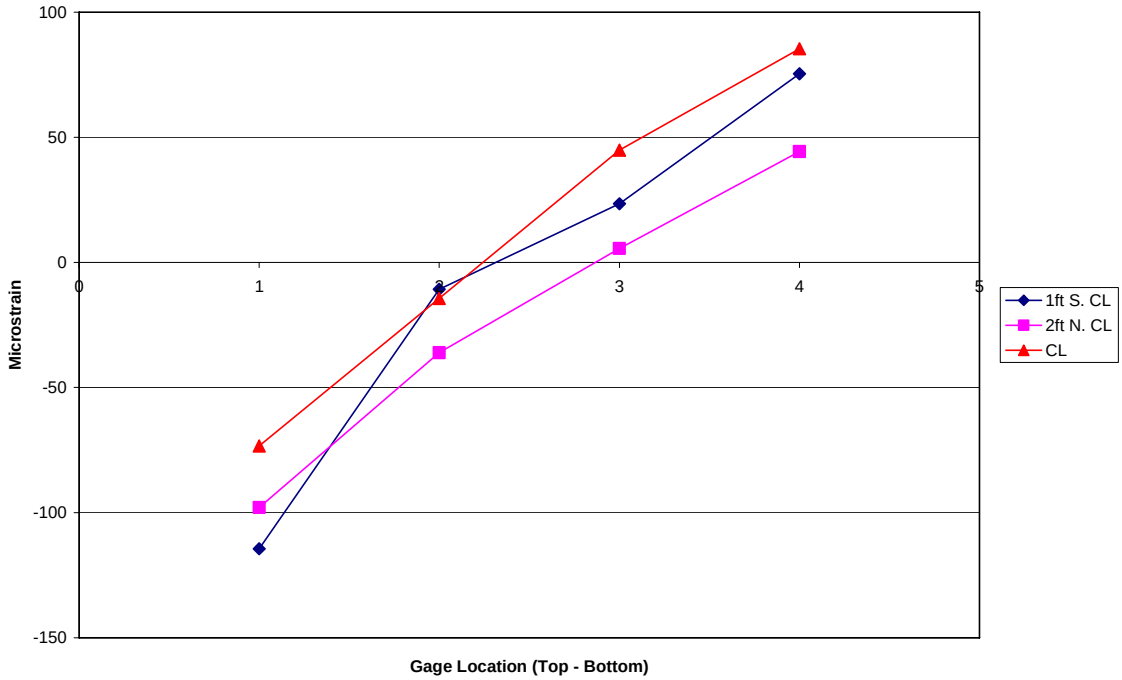

Figure 10. Side panel strain distribution, West side, LC2.